Composites Science and Technology 127 (2016) 47–53

Contents lists available at ScienceDirect

Composites Science and Technology

journal homepage: http://www.elsevier.com/locate/compscitech

Effects of tungsten disulphide nanotubes and glutaric acid on the thermal and mechanical properties of polyvinyl alcohol

Amit Kumar Sonker [a], H. Daniel Wagner [b], Reeti Bajpai [b], Reshef Tenne [b], XiaoMeng Sui [b, *]

[a] Department of Materials Science and Engineering, Indian Institute of Technology Kanpur, Kanpur 208016, India
[b] Department of Materials and Interfaces, Weizmann Institute of Science, Rehovot 7610001, Israel

ARTICLE INFO

Article history:
Received 26 November 2015
Received in revised form
18 February 2016
Accepted 19 February 2016
Available online 23 February 2016

Keywords:
Nano composites
Polymer-matrix composites
Thermal properties
Mechanical properties
Crosslinking

ABSTRACT

Polyvinyl alcohol (PVA) is a biocompatible, semi-crystalline and water soluble polymer with moderate tensile properties. To improve the thermal and mechanical properties of PVA, as well as to reduce water uptake, structural modification by glutaric acid (GA) and nanoparticle reinforcement by tungsten disulphide nanotubes (WSNTs) were used to prepare PVA based composites. We observed a significant drop in the water uptake of GA crosslinked PVA, an indication of the formation of a network. Fourier transform infrared spectroscopy was applied to confirm the presence of covalent bonds formed during the crosslinking. Crosslinked PVA and composites are found to have higher thermal stability and mechanical properties compared to their un-crosslinked counterparts. Tensile tests show that the presence of WSNTs increases the strength (up to 25%), modulus (up to 120%) and toughness (up to 80%) of the pristine as well as the crosslinked PVA.

1. Introduction

Polyvinyl alcohol (PVA) is a well-known biocompatible polymer, and it can be used in pervaporation systems [1,2], biomedical applications [3,4], and drug delivery [5–7] etc. PVA is obtained by the hydrolysis of poly (vinyl acetate), and it has a large number of hydroxyl groups [8]. Because of the abundant hydroxyl groups, PVA is a water soluble polymer, which prevents PVA from being used in a variety of potential applications where its integrity could be jeopardized, *e.g.* by moisture uptake. Crosslinking is a process that can modify the structure of polymers, and consequently affects the surface, thermal and mechanical properties of polymers [9]. PVA can be crosslinked by physical and chemical methods [9]. PVA was physically crosslinked by freezing/thawing [10] and heat treatment [11–13]. Chemically, PVA can be crosslinked by introducing a chemical agent that has good reactivity with functional groups of the polymer. For example, PVA has been modified to overcome the problem of high water absorption by cross linking with different agents such as dialdehydes, dicarboxylic acids, tricarboxylic acids, diisocyanates and inorganic acids [1,2,14–23].

Furthermore, the mechanical properties of polymers can also be improved with nano reinforcement, such as carbon nanotubes (CNTs) or WSNTs. WSNT was discovered in 1992 [24], and it has excellent mechanical properties (Young's Modulus ~ 150 GPa, bending Modulus ~ 217 GPa) [25,26]. Research has shown that the mechanical, thermal and tribological properties of epoxy [27], electrospun poly (methyl methacrylate) fibres [28], poly (propylene fumarate) [29], poly (3-hydroxybutyrate) [30] and polyvinyl alcohol [31] have been improved by adding minute amount of WSNTs. Furthermore, a number of recent studies showed that WSNT is non-toxic and biocompatible [32–34]. These characteristics suggest that addition of WSNT could be used for reinforcing biocompatible polymers, which is one of the subjects of the present work.

In this study, the modification of the thermal and mechanical properties of PVA was achieved by crosslinking the polymer and by adding the WSNT. We focused on optimizing the crosslinking conditions (more specifically, the heating time), and evaluating the effect of crosslinking and addition of WSNT on the thermal and mechanical properties of PVA. The interactions between the polymer matrix and the WSNT and within the matrix, in terms of chemical bonding, will be discussed as well.

* Corresponding author.
E-mail address: xiaomeng.sui@weizmann.ac.il (X. Sui).

http://dx.doi.org/10.1016/j.compscitech.2016.02.030
0266-3538/

2. Experimental

2.1. Materials

The semi-crystalline PVA with molecular weight of about 78,000 (98 Mol. % hydrolysed) was supplied by Polysciences, Inc. The cross linking reagent, glutaric acid ($C_5H_8O_4$), linear water soluble dicarboxylic acid, (GA, purity 99%), and sodium dodecyl sulphate (SDS, purity 99%) as surfactant, were supplied by Sigma Aldrich. WSNT (purity > 95%) was purchased from NanoMaterials Ltd. The WSNTs were synthesized in a fluidized-bed reactor [35]. Typically the WSNTs diameter and average length were ~50–150 nm and 2–5 μm, respectively. It can be seen in the TEM image (insert in Fig. 2). All materials were used as-is, without further treatment.

2.2. Film preparation

Three types of PVA films were prepared, *i.e.* pristine PVA, thermally crosslinked PVA (TH-CL-PVA) and glutaric acid crosslinked PVA (GA-CL-PVA). For each type, WSNT was added as reinforcement. The nomenclature of the different samples is included in Table 1.

Films were prepared by solution casting. PVA was dissolved in deionized water at 90 °C. The solution was casted into a polystyrene petri dish and kept in an oven for 24 hours at 45 °C to evaporate water. For the TH-CL-PVA film, the dry film was peeled off and heated at 125 °C. Heating was lasted for 0.5,1, 2, 3, 4, 6, 9 and 12 hours to optimize the crosslinking process. For the GA-CL-PVA film, 30 wt.% (compared to PVA) glutaric acid was added to the initial PVA solution. The film casting and drying procedures were the same as those for the thermally crosslinked samples. In this case, heating induces the esterification reaction between the glutaric acid and the hydroxyl groups on PVA. The average thickness of the films was about 250 μm.

To prepare the WSNT reinforced samples, 1 wt.% (relative to PVA) WSNT was dispersed in water using surfactant (SDS) followed by sonication for 1 hour. The suspension was then added to PVA or PVA-GA mixture. The film casting and drying procedures were the same as for the preparation of an unreinforced sample.

As shown in Fig. 1, the PVA film is transparent in appearance, whereas the GA-CL-PVA film and WSNT-GA-CL-PVA nanocomposite film are yellow and metallic grey, respectively. The TH-CL-PVA film is also transparent (not shown here).

2.3. Characterization and tests of the films

To evaluate the water absorption of PVA films, swelling test was conducted. The swelling study was performed according to the ISO standard (ISO 62:2008, Plastics - Determination of water absorption) to observe the change in water uptake. Samples of different crosslinking time were cut into pieces of 2.5 cm × 2.5 cm, weighed and immersed into deionized water for 48 hours at room temperature. The swollen samples were wiped with tissue paper to remove excess water from the surface. These samples were then weighed to calculate the swelling percentage. In each set, 3 samples were measured.

Fourier transform infrared (FTIR) spectra of the samples were collected with Thermoscientifc Instrument (Nicolet 6700), in the frequency range 400–4000 cm^{-1}. For the FTIR measurement, each film was cut into small pieces and grinded with KBr to form a pellet. Raman spectroscopy was performed using a Renishaw Raman Spectroscope in the 180° backscattering geometry with the 632.8 nm line of a 2 mW HeNe laser. The polarized laser was focused on the specimen through an x50 objective lens, and the diameter of the laser spot was about 2 μm. X-ray diffraction (XRD) study was conducted on Ultima III (Rigaku), in the 2θ ranges from 10° to 25° at a scanning rate 1°/min. Thermogravimetric analysis (TGA) and differential thermogravimetric analysis (DTGA) of samples were performed from 25 °C to 600 °C using a TA Instrument (SDT Q 600) at a heating rate of 10 °C per minute in the presence of nitrogen gas. Scanning electron microscopy (SEM) images were taken under the Leo Supra 55 FEG, Zeiss. The applied voltage was 3 kV, and working distance of about 5 mm. Prior to the SEM examination, samples were mounted on the aluminium SEM stubs and coated with Au-Pd by sputtering to avoid charging.

For the tensile test experiments, the specimens were prepared according to ASTM D882-12 standard. The deformation rate was 10 mm/min. To avoid the influence of moisture, all the specimens were kept in an oven at 45 °C for 12 hours before the tensile test. At least 10 specimens of each type were tested.

Table 1
Nomenclature of the different PVA films.

Abbreviations	Full name
PVA	Neat polyvinyl alcohol
TH-CL-PVA	Thermally crosslinked PVA
GA-CL-PVA	Glutaric acid crosslinked PVA
WSNT-PVA	WS_2 nanotubes reinforced PVA
WSNT-TH-CL-PVA	WSNT reinforced thermally crosslinked PVA
WSNT-GA-CL-PVA	WSNT reinforced glutaric acid crosslinked PVA

3. Results and discussion

3.1. Bonds in the crosslinked composite

In a thermally crosslinked PVA sample, heating induces a dehydration reaction. Part of the hydroxyl groups participate in the dehydration reactions, and form ether bonds. This heat induced crosslinking results in the reduction of hydroxyl groups on the PVA chains, and the release of water molecules from the system. Upon the reduction of the hydroxyl groups, the PVA structure even becomes polyene [16]. The unreacted hydroxyl groups can form intramolecular or intermolecular hydrogen bonds.

The mechanism of the crosslinking by glutaric acid is an esterification reaction, in which a carboxylic group reacts with a hydroxyl group and results in ester bond. GA has a carboxylic group at each end of the molecule. The esterification may be intramolecular or intermolecular with respect to the PVA chains. The glutaric acid can react with hydroxyl groups either belonging to two different chains or to the same PVA chain. It is also possible that one carboxylic group of glutaric acid gets crosslinked with a PVA chain and the other–COOH group remains uncrosslinked, which also affects crystallinity of PVA.

When WSNT is introduced in the PVA based composite, another hydrogen bond can form between WSNT and PVA. The WSNTs are made of concentric layers of WS_2, but the structure of WS_2 tubes is more complex than that of MWCNT. The WS_2 layer contains a sublayer of metal atoms, sandwiched between two sulphur sublayers, with the metal atom bonded to six sulphur atoms in a trigonal prismatic coordination. Sulphur is a known hydrogen bonding acceptor [36] and consequently the outermost sulphur atoms of the WSNT can form hydrogen bonds with the hydroxyl groups of PVA.

Thus three chemical bonds form in the WSNT-GA-CL-PVA composite, *i.e.* hydrogen bond between PVA chains, ester bond between PVA and GA and hydrogen bond between the WSNT and PVA (Fig. 2).

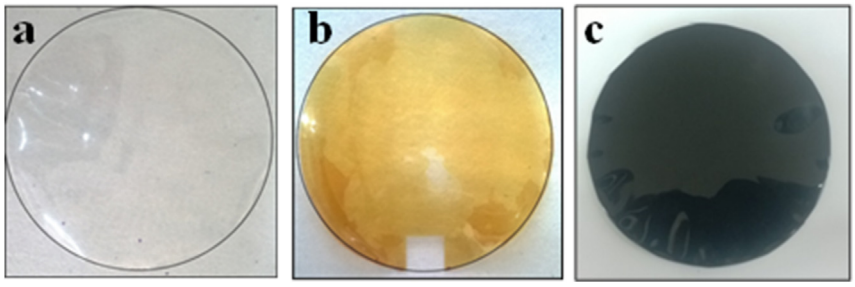

Fig. 1. (a) PVA (b) GA-CL-PVA (c) WSNT-GA-CL-PVA films.

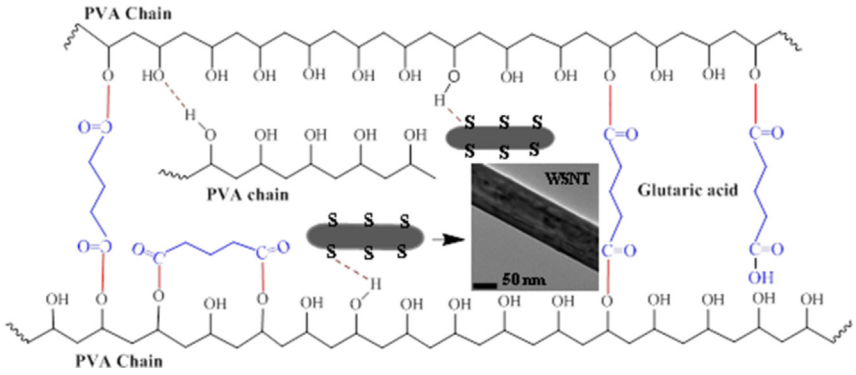

Fig. 2. Schematic drawing of the bonding in the crosslinked WSNT-PVA composite. It shows intermolecular and intramolecular ester bonds and hydrogen bonds. The drawing also illustrated the S···H–O hydrogen bonds between WSNT and PVA. Insert is the TEM image of a single WSNT, the scale bar is 50 nm.

3.2. Swelling study–water uptake

As discussed in the previous section, thermally and chemically crosslinked PVA result in the reduction of the hydroxyl groups. Consequently when immersed in water, pristine PVA and crosslinked PVA films will absorb different amounts of water, and gain weight and volume (swelling) in different levels. Swelling studies on crosslinked PVA were reported earlier by different groups [1,16]. PVA and GA-CL-PVA films were heated at 125 °C for different time periods. PVA and GA-CL-PVA films without heating process were also taken for the swelling test as control groups, and the unheated samples are denoted as 0 hour. The swelling percentage was calculated by the following formula,

$$Swelling\% = \frac{W_S - W_D}{W_D} \times 100 \quad (1)$$

where W_S and W_D are the weights of swollen and dry samples, respectively.

Fig. 3 summarizes the results of this experiment. Here we argue that (1) Short heating time results already in drastic reduction in the swelling percentage of the two samples. The non-crosslinked (0 hour) samples show the highest swelling percentages (140–150%). And the same samples present much lower swelling percentage after 0.5 h heating, *i.e.* 75% for the TH-CL-PVA and 30% for the GA-CL-PVA sample. The crosslinking leads to a reduction in the number of hydroxyl groups and consequently the water uptake of the polymer. (2) From that point onwards the swelling percentage is reduced down only slightly with the crosslinking time. The swelling percentage values are nearly the same for TH-CL-PVA and GA-CL-PVA samples when the crosslinking time exceeded two hours. Thus 2-hour was chosen as optimal crosslinking time period for sample preparation for the thermal and mechanical tests. (3) Nonetheless, the thermally crosslinked sample shows obviously

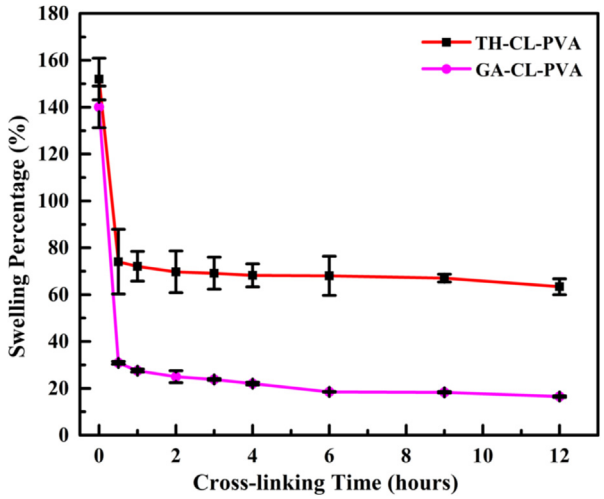

Fig. 3. Swelling percentage of TH-CL-PVA and GA-CL-PVA which were heated and crosslinked for different time periods (0.5, 1, 2, 3, 4, 6, 9 and 12 hours).

higher swelling percentage compared to the GA-CL-PVA sample. Furthermore, the reduction in the swelling percentage of heated PVA samples is temporary since it gradually absorbs moisture from the atmosphere. This phenomenon is reflected by the relatively larger error-bars of the swelling percentage of the TH-CL-PVA. Contrary to that, the swelling percentage of the GA-CL-PVA samples is much less sensitive to the ambient moisture. This is attributed to the ester bond formed between the PVA chains and the GA is more stable.

For the sake of comparison, WSNT-PVA and WSNT-GA-CL-PVA samples were also heated for two hours. The swelling percentages of all the samples are summarized in Table 2. It is found that

Table 2
Swelling percentage, crystallinity and decomposition temperature of different PVA samples.

Samples	Swelling (%)	Crystallinity (%)	Decomposition temperature (°C)
PVA	152.8 (8.9)[a]	67.4	262
TH-CL-PVA	69.7 (8.9)	75.6	264
GA-CL-PVA	24.9 (2.6)	58.5	355
WSNT-PVA	155.3 (3.6)	60.4	273
WSNT-TH-CL- PVA	73.1 (2.8)	79.4	275
WSNT-GA-CL-PVA	26.8 (4.2)	55.4	356

[a] Numbers in parenthesis are standard errors of the mean values.

WSNTs do not significantly affect the water uptake of the composite samples, even though WS_2 is somewhat hydrophilic. This can be explained first by the low content (1 wt.%) of WSNT, and second by the fact that the divalent sulphur atoms are H-bonded [36] with the PVA chains without replacing any of its hydroxyl groups.

3.3. FTIR spectroscopy

The swelling results are supported by the FTIR spectroscopy. The formation of crosslink ester bonds is confirmed by FTIR spectroscopy (Fig. 4). The FTIR spectra of PVA and TH-CL-PVA samples have −C−H stretching band (2940 cm^{-1}), −C−H bending (1435 cm^{-1}), and −C−O stretching (1095 cm^{-1}) [37]. The broad band from 3000 to 3700 cm^{-1} can be attributed to the stretching band of O−H from the intermolecular and intramolecular hydrogen bonds. Crosslinking of PVA by glutaric acid forms ester bond. As a result, the C=O stretching band at 1735 cm^{-1} and the C=C stretching band at 1670 cm^{-1} can be seen in the FTIR spectra of GA-CL-PVA samples. These two bands are marked by dashed lines in the spectra. The C=C stretching band can be detected in TH-CL-PVA samples as well, however the peak is sharper compared to the neat PVA. It is an evidence of polyene non-polar structure in the crosslinked samples.

In the FTIR spectrum of WSNT (insert in Fig. 4), the S···O−H stretching band can be observed at around 3400 cm^{-1} [31]. The presence of this band likely indicates the formation of hydrogen bond formed on the surface of WSNT. But in the FTIR spectra of WSNT based composites, this band cannot be distinguished. It is most likely that S···O−H stretching band is overlapped with the wide polymeric hydrogen bonds of PVA.

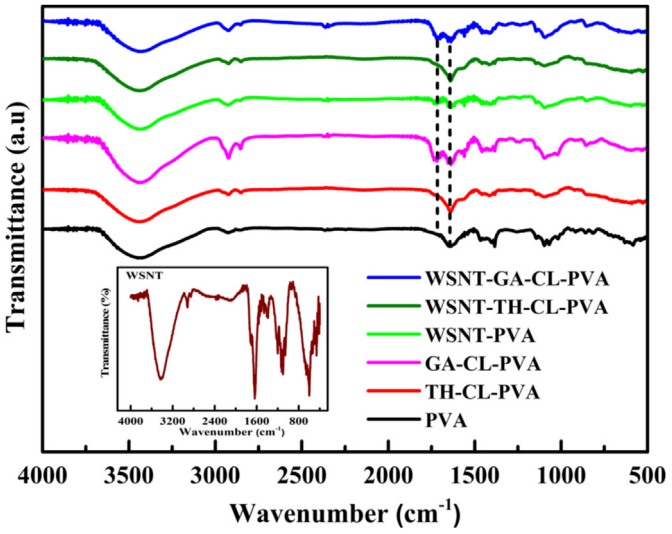

Fig. 4. FTIR spectra of different PVA samples. Insert is the FTIR spectrum of WSNT. The C=O stretching band at 1735 cm^{-1} and the C=C stretching band at 1670 cm^{-1} are marked by dashed lines.

3.4. XRD - crystallinity

XRD analysis was performed to measure the changes in the crystallinity of PVA due to the crosslinking and WSNT reinforcement. PVA is a semi-crystalline polymer with partially aligned chains. The orderly aligned chains have transplanar confirmation packed in a monoclinic unit cell [38]. PVA has one broad peak at $2\theta = 19.4°$ ($d = 4.68$ Å) with a shoulder at $2\theta = 20°$ ($d = 4.43$ Å) corresponding to the $(10\bar{1})$ and (101) reflections that emanate from the crystalline regions of atactic PVA [39,40], as shown by the dashed line on the right side of Fig. 5. The crystallinity of PVA is calculated from equation (2) [41].

$$\chi_C\% = \frac{A_C}{A_C + A_A} \times 100 \quad (2)$$

where A_C is the crystalline area and A_A is the amorphous area. And $A_C + A_A$ refers to the area under the whole XRD pattern.

Crosslinking results in the bonding of the PVA chains in an intermolecular or intramolecular manner. The changes in the molecule conformation will surely affect the crystallinity. In the case of thermally crosslinked PVA samples, the crystallinity increases as a linear polyene structure is formed. On the contrary, the GA-CL-PVA samples have lower crystallinity than their non-crosslinked counterparts (Table 1). The intramolecular crosslinking between PVA chains can reduce the crystallinity in the PVA structure. A similar decrease in the crystallinity due to intramolecular crosslinking was also observed by other research groups [1,16].

The XRD pattern of WSNT in the insert of Fig. 5 shows a sharp and narrow diffraction (002) peak of WS_2, which is located at

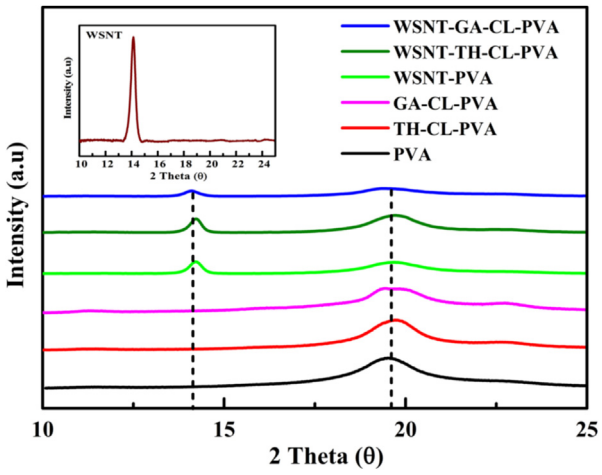

Fig. 5. XRD patterns of different PVA samples. The peaks at $2\theta = 14.2°$ and 20° (marked by dashed lines) are attributed to the WS_2 (002) peak and the crystalline PVA, respectively.

$2\theta = 14.2°$. The presence of the WSNT is confirmed by the XRD patterns of the WSNT composite samples, marked by the dashed line on the left. It is observed that the WSNT can also affect, *i.e.* decrease in most cases, the crystallinity of PVA. The WSNT-GA-CL-PVA has the lowest crystallinity among all other PVA samples. It is most likely attributed to the S···O—H hydrogen bond, which, in analogy to GA, is believed to inhibit the formation of ordered alignment of the PVA chains.

The XRD results are also supported by the tensile tests as the crystallinity of a polymer is related with its tensile properties, which will be discussed in a later section.

3.5. Thermal stability

In order to evaluate the effects of crosslinking and the WSNT reinforcing, TGA and DTGA studies were carried out to determine the changes in the thermal stability and decomposition temperature of the samples.

Fig. 6a represents TGA plots of different samples. Before discussing the results, we wish to emphasize that we will be focusing on the trend of the TGA plots, rather than the exact weight loss values which will not be discussed here. This is simply because only a small piece of the film samples (about 10 mg for each) was examined. Such small amount of the samples does not reflect the statistical weight percentage of the nanotubes reliably because the distribution of the WSNT may not be absolutely uniform. In the PVA sample, the weight loss was observed over two temperature regions, *i.e.* 25—250 °C and 300—450 °C. In the first region moisture and free water molecules were removed from the neat PVA and crosslinked PVA samples. The second region corresponds to chain scission and degradation of the PVA back bone. Crosslinked samples also show weight loss, but relatively smaller compared to those of uncrosslinked samples. This is because the 2 hours crosslinking removes all the moisture and free water molecules from the samples. In the second region, GA-CL-PVA and WSNT-GA-CL-PVA samples show significantly less weight loss in comparison to other PVA samples. This effect can be ascribed to the ester bond, which is thermally more stable than hydrogen bond.

Crosslinking modified the PVA structure, and it can be reflected in the DTGA plots in Fig. 6b. The DTGA shows the relationship of the first derivative of weight loss versus the temperature. The peaks in the graph correspond to the decomposition temperature of the samples (also summarized in Table 2). The dashed line in the DTGA plots indicates the decomposition temperature of the pristine PVA sample. The effect of thermally crosslinking on the decomposition temperature is almost negligible (2 °C). This observation is attributed to the gradual heating of the samples. Thus the uncrosslinked samples went through dehydration process as the TH-CL samples did. Among all the samples, the GA-CL-PVA samples present the highest thermal stability. The decomposition temperature of the PVA was increased by about 90 °C. Again, the higher thermal stability of the GA-CL-PVA samples is attributed to the higher stability of the ester bond.

The WSNT reinforced samples also show small shift in the decomposition temperature (about 10 °C), which can be explained by the formation of the S···O—H hydrogen bond between the WSNT and the PVA.

3.6. Mechanical properties

Since the crosslinking and WSNT reinforcing change the bonding in the PVA chains, it is expected to affect the mechanical properties. All samples were cut into strips for the tensile tests, and measured according to ASTM D882-12 standard. The results are summarized in Table 3. The modulus is the slope of the linear part of the stress-strain curve, and the toughness is simply taken as the area under the stress-strain curve.

The fracture surfaces of the samples after the tensile test were examined by SEM, as seen in Fig. 7. The SEM image in Fig. 7 shows that WSNTs are well dispersed in the PVA matrix, and there are no agglomerates of WSNTs observed in any sample. The WSNTs are marked with circles and their dimensions are comparable with those of the WSNTs on the TEM image insert (Fig. 2). Pull-out of nanotubes from the fracture surface can also be clearly observed.

Thermally crosslinked PVA and PVA composites have very high tensile strength and Young's modulus. After heat treatment, the tensile strength and modulus of PVA increase by 170% and 390%, respectively. However the elongation of the crosslinked samples decreases drastically (Fig. 8a). Since toughness is calculated by integrating the area under the stress-strain curve, a drastic decrease in elongation results in a drop in toughness. The changes in the mechanical behaviour of the TH-CL-PVA can be related to the dense network structure. The PVA chain has one hydroxyl group on every other carbon, and hydroxyl groups will partially dehydrate to form abundant ether bonds upon heating. Breaking of an ether bond requires larger energy than that necessary to break a hydrogen bond, which explains the higher strength and modulus of the TH-CL-PVA compared to the neat PVA. Along with the higher crystallinity of the crosslinked polymer, its dense network structure reduces the mobility of the PVA chains, and consequently the polymer exhibits a more brittle behaviour.

The GA-CL-PVA sample exhibits increased tensile strength (~50%), modulus (~70%) and elongation (~20%), compared to untreated PVA. The higher strength and modulus of GA-CL-PVA are

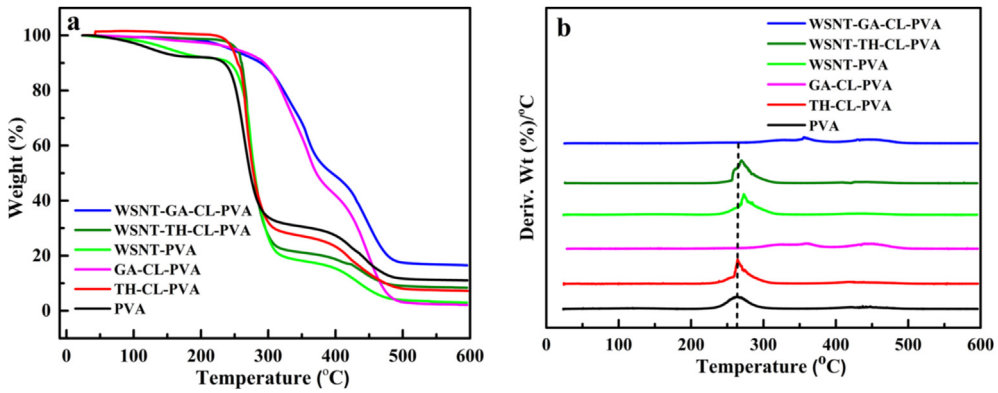

Fig. 6. (a) TGA plots of different PVA samples. (b) DTGA plot of different PVA samples. The dashed line shows the decomposition temperature of the pristine PVA.

Table 3
Summary of the tensile test results.

Samples	Elastic Modulus (GPa)	Tensile strength (MPa)	Elongation (%)	Toughness (MPa)
PVA	1.4 (0.1)[a]	44.0 (1.5)	112.5 (8.6)	42.4 (4.0)
TH-CL-PVA	7.0 (0.2)	121.6 (5.9)	2.9 (0.9)	1.8 (0.2)
GA-CL-PVA	2.4 (0.1)	66.3 (2.5)	134.5 (8.5)	62.7 (6.2)
WSNT-PVA	3.2 (0.3)	55. 5 (1. 5)	99.3 (6.4)	52.1 (4.2)
WSNT-TH-CL-PVA	7.1 (0.2)	136.9 (5.9)	3.9 (0.3)	3.3 (0.5)
WSNT-GA-CL-PVA	3.9 (0.3)	81.8 (3.1)	133.3 (11.4)	85.8 (6.4)

[a] Numbers in parenthesis are standard errors of the mean values.

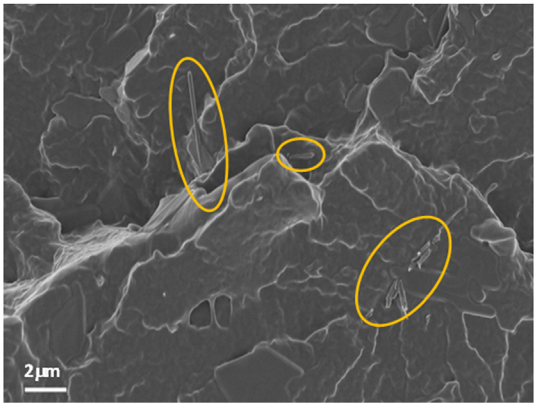

Fig. 7. SEM image of the fracture surface of the WSNT-PVA film after tensile test. The WSNTs are marked by ellipses.

the PVA samples, but reduces the strain to failure in the non-reinforced polymer, which are typical effects of reinforcement. For example, with 1 wt.% WSNT addition, the WSNT-GA-CL-PVA sample showed improved tensile strength and toughness (by 86.08% and 102.4% respectively), compared to the counterpart. The improvement is more pronounced than in the literature where PVA was reinforced with 2D MoS_2 and WS_2 nanosheets [31]. This observation suggests that the interfacial interaction s between the WS_2 nanotubes and the PVA is quite strong, and the stress is transferred effectively from the polymer matrix to the reinforcing material. This is rationalized by the abundance of hydrogen bonds formed between the WS_2 nanotubes and the PVA.

4. Conclusions

In this work, the effects of glutaric acid crosslinking and WSNTs reinforcement on the thermal and mechanical properties of PVA

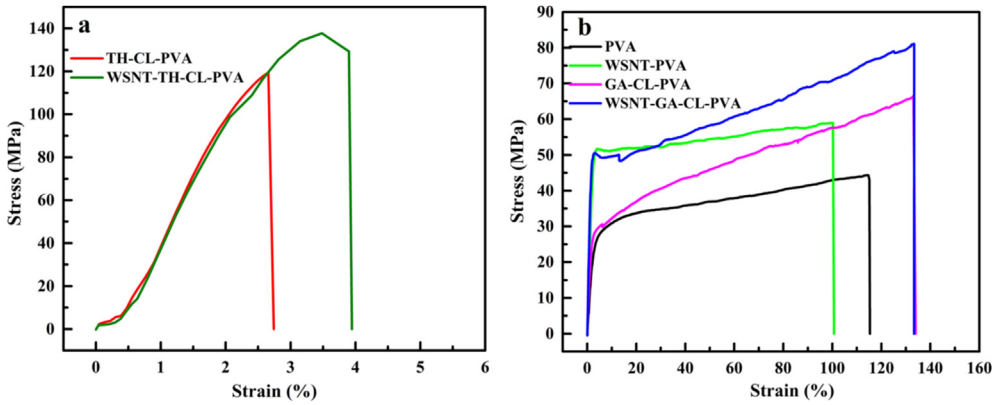

Fig. 8. Typical stress-strain curves of (a) thermally crosslinked PVA and WSNT-PVA films, and of (b) PVA, WSNT-PVA films without crosslinking and PVA, WSNT-PVA films crosslinked by glutaric acid.

due to the formation of network between the PVA chains. Given the higher strength and elongation, the GA-CL-PVA exhibits the highest toughness of all the tested samples. In the chemically crosslinked PVA, the glutaric acid crosslinker has a relatively short chain (3-carbon backbone) and one carboxyl group on each end. The crosslinking can happen either in an intermolecular or intra-molecular fashion. Lower crystallinity can result in higher polymer ductility. At the same time the intermolecular crosslinking can increase the length of the polymer chain, which means higher mobility in the plastic region. As a result the GA-CL-PVA exhibits higher strain at failure. It should also be noted that in PVA and GA-CL-PVA samples, the alignment of the polymer chains increases due to the intensive stretching, therefore the more ductile pristine and GA-CL-PVA samples show strong strain hardening effect.

The addition of WS_2 nanotubes raises the strength and moduli of

were demonstrated. The crosslinking of PVA was achieved by a chemical reaction with glutaric acid, or by heating. FTIR spectroscopy confirmed the formation of ester bonds when GA is applied. Swelling study showed that crosslinked PVA samples have 6 fold less water uptake than pristine PVA samples. Crosslinked PVA samples have higher tensile strength, modulus and toughness in comparison to PVA. The crosslinked samples were more stable at high temperatures. Even with a small amount, WSNT reinforcement showed remarkably enhanced mechanical properties for both PVA and crosslinked PVA, with little effect on the thermal properties. Our work has shown that the combination of GA crosslinking and the reinforcement effect of the bio-compatible WS_2 nanotubes could be a good methodology for improving the performance of PVA. WS_2 is also known as solid lubricant, thus composite samples will be examined in the future to assess any possible tribological

effects due to the added WSNT.

Acknowledgements

The authors would like to acknowledge support from the INNI Focal Technology Area program “Inorganic nanotubes (INT): from nanomechanics to improved nanocomposites”, as well as from the G.M.J. Schmidt Minerva Centre of Supramolecular Architectures at the Weizmann Institute. This research was also made possible in part by the generosity of the Harold Perlman family. H.D.W. is the recipient of the Livio Norzi Professorial Chair in Materials Science.

References

[1] M. Heydari, A. Moheb, M. Ghiaci, M. Masoomi, Effect of cross-linking time on the thermal and mechanical properties and pervaporation performance of poly(vinyl alcohol) membrane cross-linked with fumaric acid used for dehydration of isopropanol, J. Appl. Polym. Sci. 128 (2013) 1640–1651.
[2] N. Işıklan, O. Şanlı, Separation characteristics of acetic acid–water mixtures by pervaporation using poly(vinyl alcohol) membranes modified with malic acid, Chem. Eng. Process 44 (2005) 1019–1027.
[3] S.V. Caro, C.S.P. Sung, E.W. Merrill, Reaction of hexamethylene diisocyanate with polyvinyl-alcohol) films for biomedical applications, J. Appl. Polym. Sci. 20 (1976) 3241–3246.
[4] F. Arranz, M. Sánchez-Chaves, R. Martínez, Reaction of poly(vinyl alcohol) with n-butyl isocyanate. Chemical hydrolysis of the resulting polymers, Angew. Makromol. Chem. 152 (1987) 79–91.
[5] F. Arranz, E.M. Bejarano, M. Sanchez-Chaves, Poly(vinyl alcohol) functionalized by chloroacetate groups. Coupling of bioactive carboxylic acids, Macromol. Chem. Phys. 195 (1994) 3789–3798.
[6] F. Arranz, M. Sanchezchaves, A. Molinero, Poly(vinyl-alcohol) modification with normal-alkyl chloroformates, Angew. Makromol. Chem. 112 (1983) 205–215.
[7] R.S. Langer, N.A. Peppas, Present and future applications of biomaterials in controlled drug delivery systems, Biomaterials 2 (1981) 201–214.
[8] F. Horii, K. Masuda, in: A. Isao, A. Tetsou (Eds.), Studies in Physical and Theoretical Chemistry, Elsevier, 1998, pp. 713–736.
[9] B. Bolto, T. Tran, M. Hoang, Z. Xie, Crosslinked poly(vinyl alcohol) membranes, Prog. Polym. Sci. 34 (2009) 969–981.
[10] A.S. Hickey, N.A. Peppas, Mesh size and diffusive characteristics of semicrystalline poly(vinyl alcohol) membranes prepared by freezing/thawing techniques, J. Membr. Sci. 107 (1995) 229–237.
[11] M.G. Katz, T. Wydeven, Selective permeability of PVA membranes. II. Heat-treated membranes, J. Appl. Polym. Sci. 27 (1982) 79–87.
[12] A. Amanda, S.K. Mallapragada, Comparison of protein fouling on heat-treated poly(vinyl alcohol), poly(ether sulfone) and regenerated cellulose membranes using diffuse reflectance infrared fourier transform spectroscopy, Biotechnol. Prog. 17 (2001) 917–923.
[13] Y.L. Wang, H. Yang, Z.L. Xu, Influence of post-treatments on the properties of porous poly(vinyl alcohol) membranes, J. Appl. Polym. Sci. 107 (2008) 1423–1429.
[14] K.C.S. Figueiredo, T.L.M. Alves, C.P. Borges, Poly(vinyl alcohol) films cross-linked by glutaraldehyde under mild conditions, J. Appl. Polym. Sci. 111 (2009) 3074–3080.
[15] E. Campos, P. Coimbra, M.H. Gil, An improved method for preparing glutaraldehyde cross-linked chitosan–poly(vinyl alcohol) microparticles, Polym. Bull. 70 (2013) 549–561.
[16] J.M. Gohil, A. Bhattacharya, P. Ray, Studies on the crosslinking of poly (vinyl alcohol), J. Polym. Res. 13 (2006) 161–169.
[17] R.Y.M. Huang, J.W. Rhim, Modification of poly(vinyl alcohol) using maleic acid and its application to the separation of acetic acid-water mixtures by the pervaporation technique, Polym. Int. 30 (1993) 129–135.
[18] J.-W. Rhim, H.B. Park, C.-S. Lee, J.-H. Jun, D.S. Kim, Y.M. Lee, Crosslinked poly(vinyl alcohol) membranes containing sulfonic acid group: proton and methanol transport through membranes, J. Membr. Sci. 238 (2004) 143–151.
[19] J. She, X.M. Shen, Crosslinked PVA-PS thin-film composite membrane for reverse osmosis, Desalination 62 (1987) 395–403.
[20] D.S. Dlamini, J. Wang, A.K. Mishra, B.B. Mamba, E.M.V. Hoek, Effect of cross-linking agent chemistry and coating conditions on physical, chemical, and separation properties of pva-psf composite membranes, Sep. Sci. Technol. 49 (2013) 22–29.
[21] M. Krumova, D. López, R. Benavente, C. Mijangos, J.M. Pereña, Effect of crosslinking on the mechanical and thermal properties of poly(vinyl alcohol), Polymer 41 (2000) 9265–9272.
[22] T. Miyazaki, Y. Takeda, S. Akane, T. Itou, A. Hoshiko, K. En, Role of boric acid for a poly (vinyl alcohol) film as a cross-linking agent: melting behaviors of the films with boric acid, Polymer 51 (2010) 5539–5549.
[23] C.K. Yeom, R.Y.M. Huang, Pervaporation separation of aqueous mixtures using crosslinked poly(vinyl alcohol), I. Characterization of the reaction between PVA and amic acid, Angew. Makromol. Chem. 184 (1991) 27–40.
[24] R. Tenne, L. Margulis, M. Genut, G. Hodes, Polyhedral and cylindrical structures of tungsten disulphide, Nature 360 (1992) 444–446.
[25] I. Kaplan-Ashiri, S.R. Cohen, K. Gartsman, V. Ivanovskaya, T. Heine, G. Seifert, I. Wiesel, H.D. Wagner, R. Tenne, On the mechanical behavior of WS2 nanotubes under axial tension and compression, Proc. Natl. Acad. Sci. 103 (2006) 523–528.
[26] M. Wang, I. Kaplan-Ashiri, X. Wei, R. Rosentsveig, H. Wagner, R. Tenne, L. Peng, In situ TEM measurements of the mechanical properties and behavior of WS2 nanotubes, Nano Res. 1 (2008) 22–31.
[27] E. Zohar, S. Baruch, M. Shneider, H. Dodiuk, S. Kenig, R. Tenne, H.D. Wagner, The effect of WS2 nanotubes on the properties of epoxy-based nanocomposites, J. Adhes. Sci. Technol. 25 (2011) 1603–1617.
[28] C.S. Reddy, A. Zak, E. Zussman, WS2 nanotubes embedded in PMMA nanofibers as energy absorptive material, J. Mater. Chem. 21 (2011) 16086–16093.
[29] G. Lalwani, A.M. Henslee, B. Farshid, P. Parmar, L. Lin, Y. Qin, F.K. Kasper, A.G. Mikos, B. Sitharaman, Tungsten disulfide nanotubes reinforced biodegradable polymers for bone tissue engineering, Acta Biomater. 9 (2013) 8365–8373.
[30] M. Naffakh, C. Marco, G. Ellis, S.R. Cohen, A. Laikhtman, L. Rapoport, A. Zak, Novel poly(3-hydroxybutyrate) nanocomposites containing WS2 inorganic nanotubes with improved thermal, mechanical and tribological properties, Mater. Chem. Phys. 147 (2014) 273–284.
[31] S.-K. Kim, J.J. Wie, Q. Mahmood, H.S. Park, Anomalous nanoinclusion effects of 2D MoS2 and WS2 nanosheets on the mechanical stiffness of polymer nanocomposites, Nanoscale 6 (2014) 7430–7435.
[32] W.Z. Teo, E.L.K. Chng, Z. Sofer, M. Pumera, Cytotoxicity of exfoliated transition-metal dichalcogenides (MoS2, WS2, and WSe2) is lower than that of graphene and its analogues, Chem. Eur. J. 20 (2014) 9627–9632.
[33] J.T. Rashkow, Y. Talukdar, G. Lalwani, B. Sitharaman, Interactions of 1D- and 2D-layered inorganic nanoparticles with fibroblasts and human mesenchymal stem cells, Nanomedicine 10 (2015) 1693–1706.
[34] M. Pardo, T. Shuster-Meiseles, S. Levin-Zaidman, A. Rudich, Y. Rudich, Low cytotoxicity of inorganic nanotubes and fullerene-like nanostructures in human bronchial epithelial cells: relation to inflammatory gene induction and antioxidant response, Environ. Sci. Technol. 48 (2014) 3457–3466.
[35] A. Zak, L. Sallacan-Ecker, A. Margolin, M. Genut, R. Tenne, Insight into the growth mechanism of WS2 nanotubes in the scaled-up fluidized-bed reactor, Nano 04 (2009) 91–98.
[36] D.L. Howard, H.G. Kjaergaard, Hydrogen bonding to divalent sulfur, Phys. Chem. Chem. Phys. 10 (2008) 4113–4118.
[37] E.R. Blout, R. Karplus, The infrared spectrum of polyvinyl alcohol, J. Am. Chem. Soc. 70 (1948) 862–864.
[38] C.W. Bunn, Crystal structure of polyvinyl alcohol, Nature 161 (1948) 929–930.
[39] H.E. Assender, A.H. Windle, Crystallinity in poly(vinyl alcohol). 1. An X-ray diffraction study of atactic PVOH, Polymer 39 (1998) 4295–4302.
[40] R.C.L. Mooney, An X-ray study of the structure of polyvinyl alcohol, J. Am. Chem. Soc. 63 (1941) 2828–2832.
[41] L.E. Alexander, X-ray Diffraction Methods in Polymer Science, Wiley-Interscience, New York, 1970.